EPJ Web of Conferences **60**, 08003 (2013)
DOI: 10.1051/epjconf/20136008003

Diboson Production at LHC and Tevatron

Pat Ward[1,a] on behalf of the ATLAS, CMS, CDF and D0 Collaborations

[1] *University of Cambridge*

Abstract. Measurements of the production of pairs of gauge bosons by the ATLAS and CMS experiments at the LHC and the CDF and D0 experiments at the Tevatron are summarized. Measured cross-sections are generally consistent with Standard Model predictions calculated at next-to-leading order in QCD. Transverse momentum distributions of bosons or leptons produced in these processs have been used to set limits on anomalous triple gauge boson couplings. Limits on $WW\gamma$ and WWZ anomalous couplings are approaching, or exceeding, those derived from measurements at LEP, while those on neutral couplings are an order of magnitude more stringent than limits from LEP. First limits on anomalous quartic gauge boson couplings from the Tevatron and LHC are also presented.

1 Introduction

Measurements of the production of pairs of gauge bosons in high-energy pp and $p\bar{p}$ collisions probe triple gauge boson couplings, and hence provide a sensitive test of the gauge structure of the Standard Model (SM). Deviations of the vector-boson couplings from their SM values (anomalous triple gauge boson couplings, aTGCs) would be an indication of new physics at a higher energy scale. Non-resonant production of WW and ZZ pairs forms an irreducible background to the newly-discovered Higgs boson candidate [1, 2] which must be understood in order to study the properties of this particle. In addition, new particles predicted by e.g. Technicolor models may decay into pairs of gauge bosons.

Diboson production in $p\bar{p}$ collisions at a centre-of-mass energy $\sqrt{s}$ = 1.96 TeV has been measured by the CDF [3] and D0 [4] experiments at the Tevatron using data samples with an integrated luminosity up to 9.7 fb^{-1}. At the LHC, ATLAS [5] and CMS [6] have made comprehensive measurements using ~5 fb^{-1} of pp collision data at $\sqrt{s}$ = 7 TeV collected in 2011, and first cross-sections have been measured using up to 20 fb^{-1} of integrated luminosity at $\sqrt{s}$ = 8 TeV collected in 2012. This talk summarizes these cross-section measurements, and the limits on aTCGs which have been derived from them. In addition, first limits from the Tevatron and LHC on anomalous quartic gauge boson couplings are presented.

2 Cross-section Measurements

Cross-sections for diboson production are two or three orders of magnitude lower than those for single boson production, which forms the major background source in most channels. Measurements have mainly been performed in the leptonic decay channels of the W and Z bosons, i.e. $W \to \ell\nu$ and $Z \to \ell\ell$ where ℓ signifies an electron or muon. While these channels have low branching ratios, they have experimentally clean signatures. W bosons are selected by requiring a high transverse momentum (p_{T}) lepton, significant missing transverse momentum ($E_{\mathrm{T}}^{\mathrm{miss}}$) from the neutrino, and a requirement on the W boson transverse mass reconstructed from the charged lepton and missing transverse momentum. Z bosons are selected by requiring a same-flavour opposite-charge dilepton pair with an invariant mass near the Z-boson mass. The exact mass range used, in both the experimental selection and in the definition of the cross-section measured, varies from experiment to experiment. Important background contributions are estimated using data-driven techniques wherever possible.

Measured cross-sections are compared to the corresponding theoretical predictions provided by each experiment. These are calculated at next-to-leading order (NLO) in QCD. Uncertainties arising from missing higher-order terms, assessed by varying the renormalization and factorization scales, and from parton density functions, are estimated to be $O(5\%)$.

2.1 $W\gamma$ and $Z\gamma$

$W\gamma$ and $Z\gamma$ production have been measured by ATLAS [7] and CMS [8, 9] at $\sqrt{s}$ = 7 TeV. In the $\ell\nu\gamma$ and $\ell\ell\gamma$ final states the measurements are performed for photon transverse momentum E_{T}^{γ} >15 GeV, and require $\Delta R(\ell, \gamma) > 0.7$ to suppress the contribution from final-state radiation from the charged lepton(s). In the $\nu\nu\gamma$ final state the photon transverse energy is required to be above 100 GeV (145 GeV) in ATLAS (CMS) to suppress background from W boson and γ+jets production. Measurements of differential cross-sections for $W\gamma$ and $Z\gamma$ production from AT-

[a] e-mail: cpw1@hep.phy.cam.ac.uk

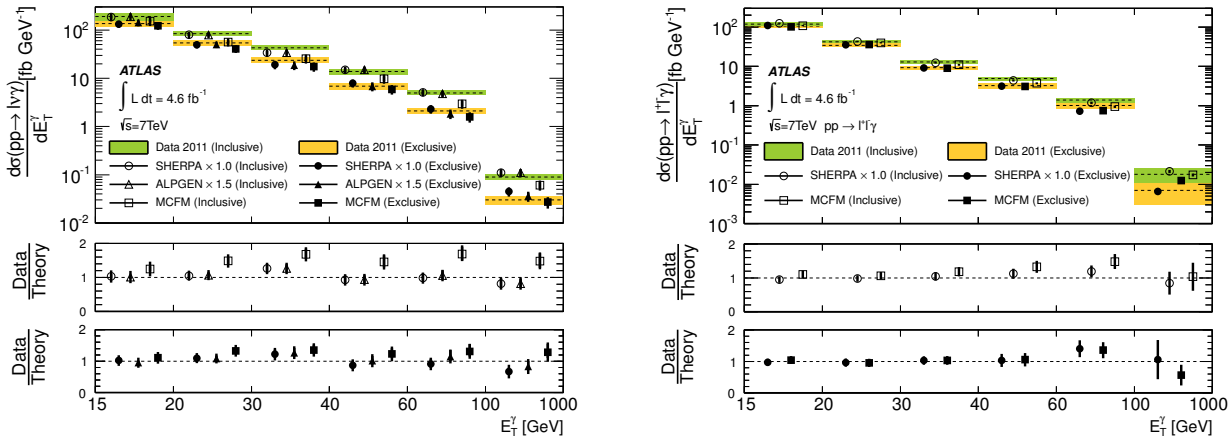

Figure 1. Differential cross-sections as a function of photon transverse momentum, E_{T}^{γ}, of (a) the $pp \to \ell\nu\gamma$ process and (b) the $pp \to \ell\ell\gamma$ process, measured by the ATLAS experiment [7]. The measurements are performed in a restricted kinematic phase-space [7] for inclusive ($N_{\mathrm{jet}} \geq 0$) and exclusive ($N_{\mathrm{jet}} = 0$) selections. The lower plots show the ratio of the data to the predictions of different generators. The cross-section predictions of the SHERPA and ALPGEN generators have been scaled by a global factor to match the total number of events observed in data. No global factor is applied to MCFM predictions.

LAS are shown in Fig. 1. In addition to inclusive measurements, ATLAS also measures exclusive cross-sections, for events with no jet with $p_{\mathrm{T}} > 30$ GeV within $|\eta| < 4.4$. The measurements are compared with NLO predictions from MCFM [10]. The agreement is good for low E_{T}^{γ}, but the $W\gamma$ data lie above the MCFM prediction for higher E_{T}^{γ}, especially for the inclusive case. This may be attributed to the fact that the jet multiplicity is observed to increase with E_{T}^{γ}, and multiple quark/gluon production is not included in the MCFM prediction. The data are also compared with predictions from the leading-order event generators ALPGEN [11] and SHERPA [12], normalized to the measured total cross-section; the shape of the E_{T}^{γ} spectra are well-reproduced by these generators.

2.2 *WW* and *WZ*

Measured cross-sections for WW production using the fully leptonic decay channel from ATLAS and CMS are compared with the corresponding SM predictions in Fig. 2(a). The uncertainties on these measurements (7–8% excluding luminosity) are dominated by systematic uncertainties, which arise primarily from the use of a jet veto in the event selection to suppress $t\bar{t}$ background, uncertainties in the remaining background, and uncertainties in lepton reconstruction and identification efficiencies. The measured cross-sections are 10–20% above the SM predictions; the predictions do not include the contribution from Higgs boson production, which is expected to be ~3(4)% at 7(8) TeV. Kinematic distributions measured in WW events are in good agreement with expectations, as illustrated in Fig. 2(b), which shows the dilepton p_{T} spectrum of the events selected by CMS at $\sqrt{s} = 8$ TeV, normalised to the measured cross-section.

Measured cross-sections for WZ production in the fully leptonic channel from the Tevatron and LHC experiments are compared with SM predictions in Fig. 3. In this channel, statistical and systematic uncertainties are similar for the LHC measurements. The measured values are in agreement with expectation.

Cross-sections for the sum of WW and WZ production have also been measured in the $\ell\nu q\bar{q}$ final state, using events with a reconstructed W boson and two hadronic jets. This channel has a higher branching ratio than the leptonic channel, but suffers from a very large background, mainly W/Z+jets events. For example, in the ATLAS measurement, in the dijet mass range of 60–120 GeV the signal fraction is 2.7%. The signal is extracted by fitting the dijet mass spectrum. The dijet mass resolution is not sufficient to distinguish W from Z, so the sum of the WW and WZ cross-sections is determined. Measured values are in good agreeement with SM predictions, as shown in Fig. 3(b).

2.3 *ZZ*

Production of pairs of Z bosons has been measured in the final state with four charged leptons, which has a low branching ratio but is experimentally very clean, and in the final state with two charged leptons and two neutrinos, which has a higher branching ratio but large background from Z+jets and WZ events. The D0 experiment has recently updated their results in the four-lepton channel, using increased luminosity and increased acceptance in the four-electron final state [26]. Both ATLAS and CMS have measured $ZZ \to 4\ell$ production at $\sqrt{s} =$ 8 TeV [15, 27]. The CMS measurement, using 5.3 fb^{-1}of data, includes final states with hadronically decaying τ leptons. The ATLAS measurement uses the full 8 TeV data sample; the invariant mass distribution of the four-lepton system is shown in Fig. 4(a). Measurements of the total cross-section are compared with theoretical predictions in Fig. 4(b), and are in good agreement with expectations. In this channel, statistical errors are dominant for all measurements.

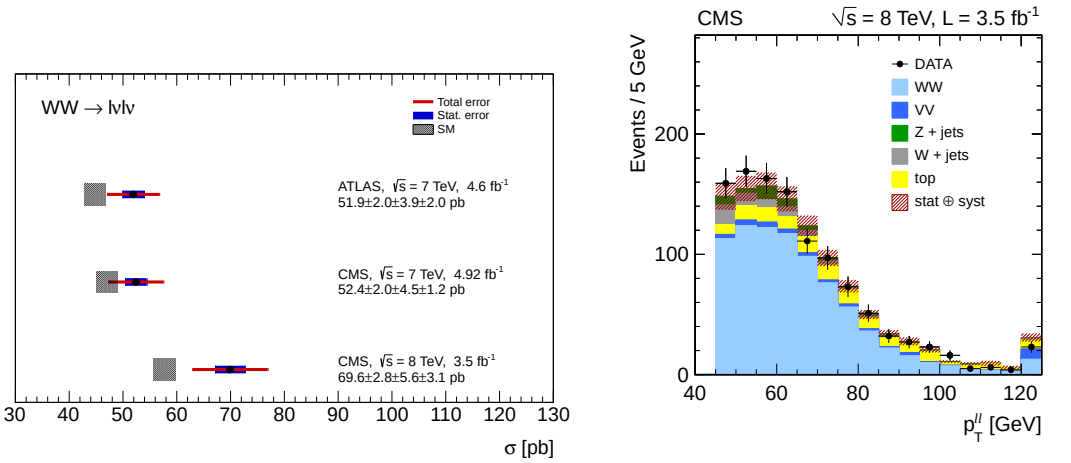

(a) (b)

Figure 2. (a) Measured values of the WW cross-section from ATLAS [13] and CMS [14, 15] compared with the SM predictions. (b) Distribution of the dilepton transverse momentum $p_{\mathrm{T}}^{\ell\ell}$ for WW candidate events in CMS data at $\sqrt{s} = 8$ TeV [15]. Points represent the data, and shaded histograms represent the WW signal and the background processes. The last bin includes the overflow. The WW signal is scaled to the measured cross-section, and the background processes are normalized to the corresponding estimated values.

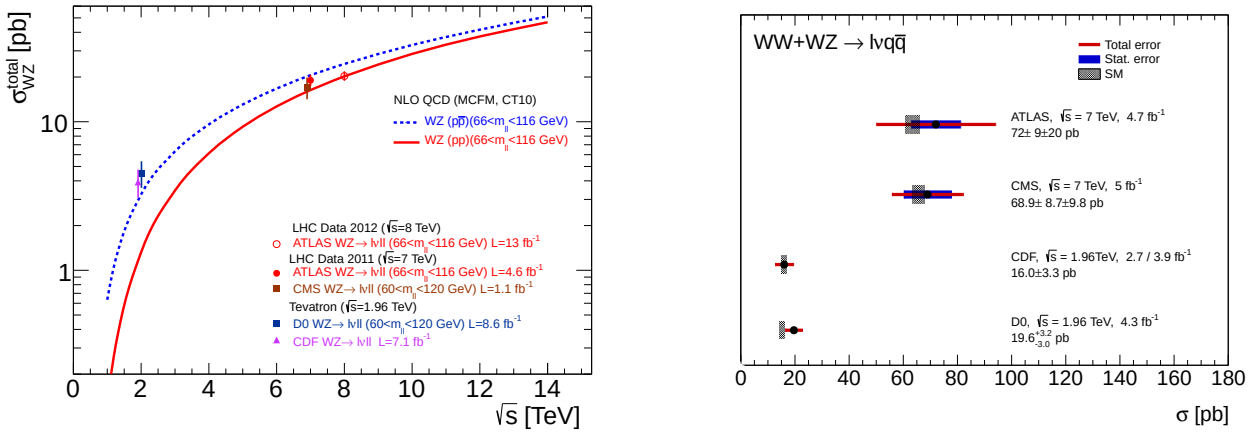

(a) (b)

Figure 3. (a) Measurements and theoretical predictions of the total WZ production cross-section as a function of centre-of-mass energy. Experimental measurements from CDF [16] and D0 [17] in $p\bar{p}$ collisions at $\sqrt{s} = 1.96$ TeV, from ATLAS [18] and CMS [19] in pp collisions at $\sqrt{s} = 7$ TeV and from ATLAS [20] at $\sqrt{s} = 8$ TeV are shown. The blue dashed (solid red) line shows the theoretical prediction for the WZ production cross-section in $p\bar{p}$ (pp) collisions, calculated at NLO using MCFM with PDF set CT10 [21]. The ATLAS results define the total cross-section with a Z boson with mass between 66 GeV and 116 GeV. The results from CDF define the total cross-section assuming zero-width for the Z boson and neglecting the γ^* contribution. The results from D0 and CMS define the total cross-section with a Z boson with mass between 60 GeV and 120 GeV. (b) Measured values of the $WW + WZ$ cross-section from measurements of the $\ell\nu q\bar{q}$ final state compared with SM predictions. Measurements from ATLAS [22] and CMS [23] in pp collisions at $\sqrt{s} = 7$ TeV and CDF [24] and D0 [25] in $p\bar{p}$ collisions at $\sqrt{s} = 1.96$ TeV are shown.

3 Limits on Anomalous Triple Gauge Boson Couplings

Diboson production probes triple gauge boson couplings which (may) contribute to the cross-section via the s-channel production diagram. These couplings are a fundamental prediction of the SM. At tree level, the couplings involving charged gauge bosons are non-zero, whereas the neutral couplings are zero. Non-SM couplings are usually introduced in an effective Lagrangian framework. Limits have been set on the aTGC parameters listed in Table 1.

For the $WW\gamma$ and WWZ vertices, these are the couplings which separately conserve charge conjugation (C) and parity (P). The $Z\gamma$ final state has been used to probe two CP-conserving couplings for each of the $ZZ\gamma$ and $Z\gamma\gamma$ vertices. The ZZ final state probes f_4^Z and f_4^γ which violate CP and f_5^Z and f_5^γ which conserve CP. Sufficiently large anomalous couplings would cause cross-sections to violate unitarity at high energies. To avoid this, a form-factor may be introduced to suppress the coupling at high energy, i.e. a coupling f takes the form $f(\hat{s}) = f(0)/(1+\hat{s}/\Lambda^2)^n$ where

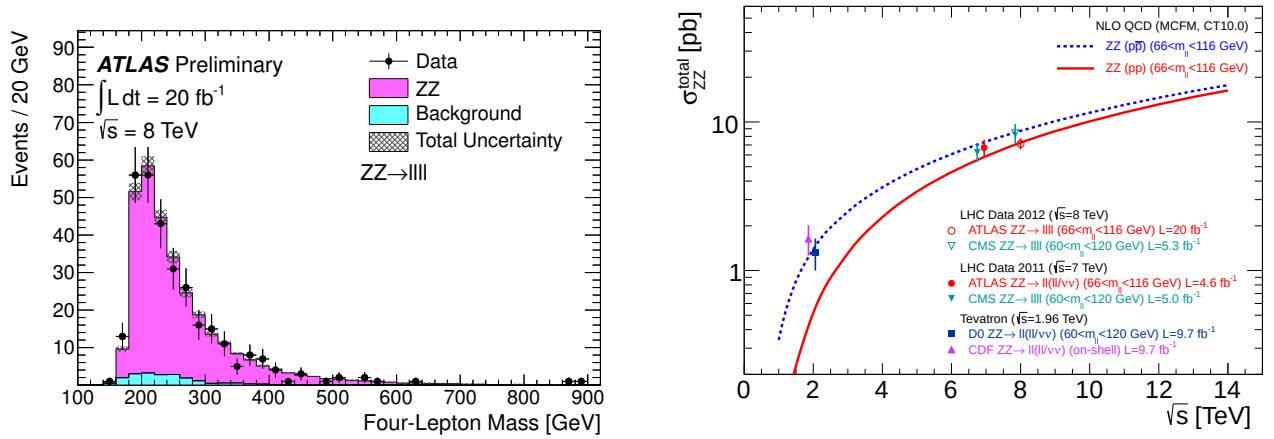

(a) (b)

Figure 4. (a) Distribution of invariant mass of the four-lepton system in $ZZ \to \ell\ell\ell\ell$ candidate events in ATLAS data at $\sqrt{s} = 8$ TeV [27]. The points show the data, while the histograms show the signal and background predictions from Monte Carlo. (b) Measurements and theoretical predictions of the total ZZ production cross-section as a function of centre-of-mass energy. Experimental measurements from CDF [28] and D0 [26] in $p\bar{p}$ collisions at $\sqrt{s} = 1.96$ TeV, from ATLAS [27, 29] and CMS [15, 30] in pp collisions at $\sqrt{s} = 7$ TeV and $\sqrt{s} = 8$ TeV are shown. The blue dashed (red solid) line shows the theoretical prediction for the ZZ production cross-section in $p\bar{p}$ (pp) collisions, calculated at NLO using MCFM with PDF set CT10. The ATLAS results define the total cross-section with a Z boson with mass between 66 GeV and 116 GeV. The results from CDF define the total cross-section assuming zero-width for the Z boson and neglecting the γ^* contribution. The results from D0 and CMS define the total cross-section with a Z boson with mass between 60 GeV and 120 GeV.

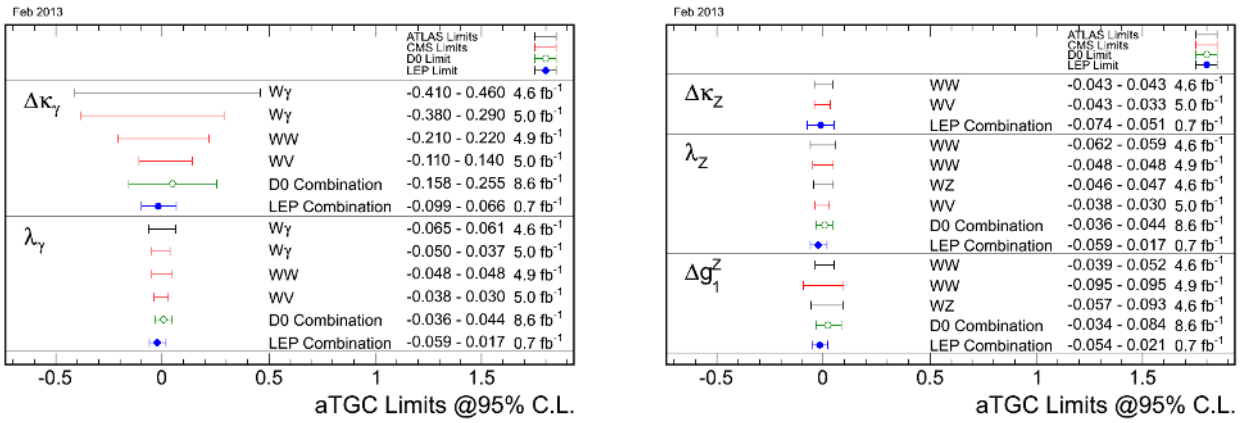

(a) (b)

Figure 5. Summary of 95% CL limits on anomalous (a) $WW\gamma$ and (b) WWZ couplings [32]. Limits on each coupling are derived assuming Standard Model values for all other couplings. Limits from LEP and the LHC are without a form factor; those from the Tevatron used a dipole form factor with $\Lambda = 2$ TeV.

$\hat{s}$ is the partonic centre-of-mass energy, Λ is the energy scale of the new physics parameterised by the anomalous coupling, and n is an integer. The Tevatron experiments usually use a dipole form factor ($n = 2$) with $\Lambda = 2$ TeV, whereas the LHC experiments prefer to quote results without a form factor.

Anomalous couplings typically increase cross-sections at high diboson invariant mass and high transverse momentum. Limits are set by fitting the transverse momentum distribution of one of the bosons, or of the leading lepton in the case of the fully leptonic WW final state. In most cases, limits have been set considering each final state separately, but D0 combine the $W\gamma$, WW and WZ channels to

Table 1. Anomalous coupling parameters measured in each diboson channel. The first column indicates the coupling, the second the parameters considered, and the third the final state(s) in which this coupling is measured.

Coupling	Parameters	Channel
$WW\gamma$	$\Delta\kappa_\gamma$, λ_γ	WW, $W\gamma$
WWZ	Δg_1^Z,$\Delta\kappa_Z$, λ_Z	WW, WZ
$ZZ\gamma$	h_3^Z, h_4^Z	$Z\gamma$
$Z\gamma\gamma$	h_3^γ, h_4^γ	$Z\gamma$
ZZZ	f_4^Z, f_5^Z	ZZ
$Z\gamma Z$	f_4^γ, f_5^γ	ZZ

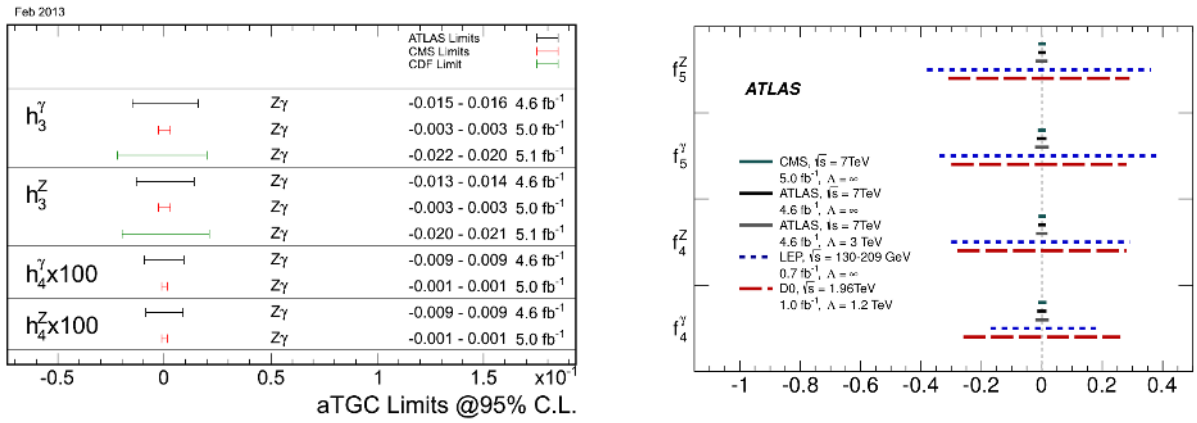

(a) (b)

Figure 6. Summary of 95% CL limits on anomalous couplings from (a) $Z\gamma$ final states [32] and (b) ZZ final states [29]. Limits on each coupling are derived assuming Standard Model values for all other couplings. For the couplings derived from $Z\gamma$, limits from the LHC are without a form factor, whereas those from CDF used a form factor with with $\Lambda = 1.5$ TeV and $n = 3(4)$ for $h_3(h_4)$.

obtain limits on the parameteres describing charged vertices [31].

Figure 5 shows a summary of limits on aTGC parameters for the $WW\gamma$ and WWZ vertices. For each parameter, the limit assumes that all other parameters have their SM values. For channels sensitive to both $WW\gamma$ and WWZ couplings, it is assumed that $\lambda_\gamma = \lambda_Z$ and $\Delta\kappa_Z = \Delta g_1^Z - \Delta\kappa_\gamma \tan^2\theta_W$. The limits from the Tevatron and LHC experiments are becoming comparable with, and in some cases improve on, those from LEP. The most stringent limit from LHC on the WWZ coupling comes from the CMS measurement of $WW + WZ \to \ell\nu q\bar{q}$ [23].

Limits on the h parameters derived from $Z\gamma$ final states and on the f parameters derived from ZZ final states are summarized in Fig. 6. The most stringent limits on the h parameters come from the CMS measurement of the $\nu\bar{\nu}\gamma$ final state [9]. These are more stringent than the corresponding limits from ATLAS [7], which use a similar integrated luminosity, because they are sensitive to the binning of the p_{T} spectrum: CMS uses $p_{\mathrm{T}}^\gamma > 400$ GeV whereas ATLAS uses $p_{\mathrm{T}}^\gamma > 100$ GeV for the last bin. Limits on the f parameters from the LHC experiments are a factor of ten more stringent than those from LEP and the Tevatron.

4 Limits on $WW\gamma\gamma$ couplings

First limits on anomalous $WW\gamma\gamma$ quartic couplings at the Tevatron and LHC have been reported by the D0 [33] and CMS [34] experiments respectively, using measurements of two-photon production of W boson pairs. D0 searches for events in the $e^+e^- + \not{E}_{\mathrm{T}}^{\mathrm{miss}}$ channel; after preselection, the SM expectation is only 0.1 event in 9.7 fb^{-1} of data, and a boosted decision tree is used to enhance any possible signal from anomalous quartic couplings. CMS searches for high-p_{T} $\mu^\pm e^\mp$ pairs, requiring no other tracks at the primary vertex. Two events are observed in 5.05 fb^{-1} of data at $\sqrt{s} = 7$ TeV, and the cross-section for exclusive $pp \to p^{(*)}WWp^{(*)} \to p^{(*)}\mu^\pm e^\mp p^{(*)}$ production is measured to be $2.2^{+3.3}_{-2.0}$ fb, consistent with the SM expectation of 4.0±0.7 fb. The p_{T} distributions of observed and expected events are shown in Fig. 7(a).

Assuming C and P invariance, anomalous $WW\gamma\gamma$ quartic couplings are described by two parameters, a_0^W and a_C^W. Limits on these parameters have been set using the boosted decision tree output (D0) or the number of events with $p_{\mathrm{T}}(\mu e) > 100$ GeV (CMS). Triple gauge boson couplings are assumed to take their SM values. Table 2 shows the resulting 95% CL limits, derived using a dipole form factor with $\Lambda = 500$ GeV. The limits from CMS, shown in Fig. 7(b), are two orders of magnitude more stringent than those from the OPAL experiment at LEP [35].

Table 2. 95% CL limits on $WW\gamma\gamma$ anomalous quartic couplings from D0 [33] and CMS [34], using a form factor with $\Lambda = 500$ GeV and $n = 2$.

	$\lvert a_0^W/\Lambda^2\rvert$/ GeV^{-2}	$\lvert a_C^W/\Lambda^2\rvert$/ GeV^{-2}
D0	0.0025	0.0092
CMS	0.00015	0.0005

5 Summary

Extensive measurements of diboson production have been made at the Tevatron and at LHC. Although these processes have low cross-sections, the precision of the measurements is becoming limited by systematic uncertainties in many channels. Experimental uncertainties on total cross-sections, which exceed 8% for the most precise measurements, are still larger than estimated theoretical uncertainties. Measurements are generally in reasonable agreement with SM expectations.

Diboson production measurements have been used to set limits on anomalous triple gauge boson couplings. Limits on $WW\gamma$ and WWZ couplings from the Tevatron and LHC experiments are approaching or exceeding those from LEP. Limits on neutral couplings are an order of

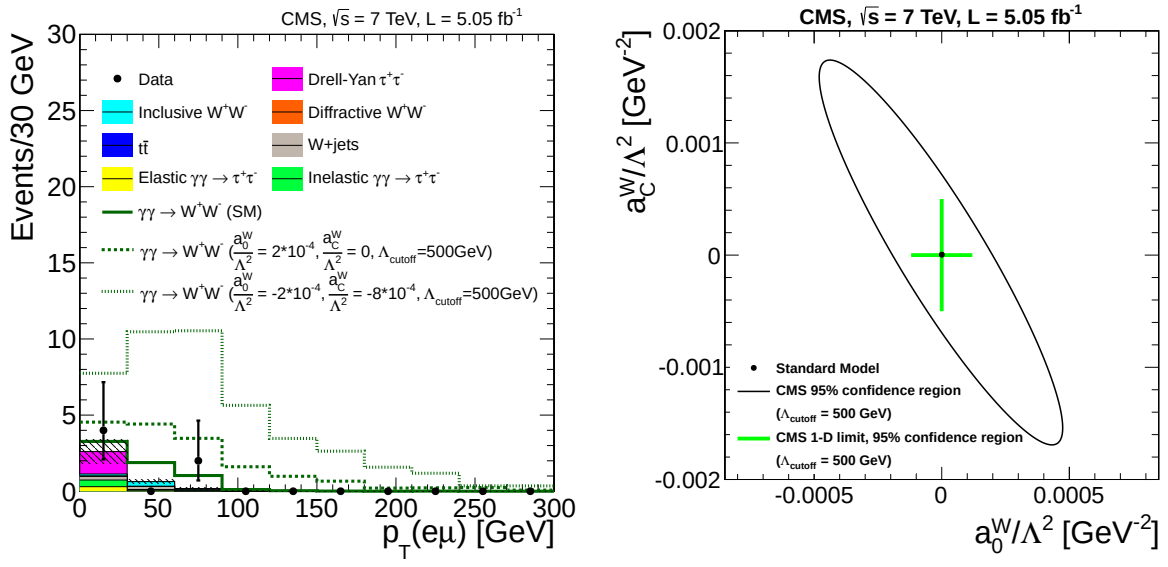

(a) (b)

Figure 7. (a) p_{T} distribution for events selected as $\gamma\gamma \to WW$ by CMS [34]. The background sources (solid histograms) are stacked with statistical uncertainties indicated by the shaded region, the signal histogram (open histogram) is stacked on top of the background. The expected signal is shown for the SM $\gamma\gamma \to WW$ signal (solid line), and for two representative values of the anomalous couplings a_0^W/Λ^2 and a_C^W/Λ^2 (dotted and dashed lines). (b) Excluded values of the anomalous coupling parameters $a_0^{\mathrm{W}}/\Lambda^2$ and $a_{\mathrm{C}}^{\mathrm{W}}/\Lambda^2$ from the measurement of two-photon production of W pairs by the CMS experiment [34].

magnitude more stringent than those from LEP. First limits on anomalous quartic couplings from the LHC are two orders of magnitude more stringent than those from LEP.

References

[1] ATLAS Collaboration, Phys. Lett. B **716** 1 (2012).
[2] CMS Collaboration, Phys. Lett. B **716** 30 (2012).
[3] CDF Collaboration, F. Abe et al., Nucl. Inst. Meth. A **271** 387 (1988).
[4] D0 Collaboration, V. M. Abazov et al., Nucl. Instrum. Meth. A **565** 463 (2006).
[5] ATLAS Collaboration, JINST **3** S08003 (2008).
[6] CMS Collaboration, JINST **3** S08004 (2008).
[7] ATLAS Collaboration, Phys. Rev. D **87** 112003 (2013).
[8] CMS Collaboration, CMS PAS EWK-11-009, http://cdsweb.cern.ch/record/1537415.
[9] CMS Collaboration, CMS PAS SMP-12-020, http://cdsweb.cern.ch/record/1532433.
[10] J. M. Campbell, R. Ellis and C. Williams, JHEP **1107** 018 (2011).
[11] M. L. Mangano et al., JHEP **0307** 001 (2003).
[12] T. Gleisberg et al., JHEP **0402** 056 (2004).
[13] ATLAS Collaboration, Phys. Rev. D **87** 112001 (2013).
[14] CMS Collaboration, arXiv:1306.1126 [hep-ex].
[15] CMS Collaboration, Phys. Lett. B **721**, 190 (2013).
[16] CDF Collaboration, T. Aaltonen et al., Phys. Rev. D **86** 031104 (2012).
[17] D0 Collaboration, V. M. Abazov et al., Phys. Rev. D **85** 112005 (2012).
[18] ATLAS Collaboration, Eur. Phys. J. C **72** 2173 (2012).
[19] CMS Collaboration, CMS PAS EWK-11-010, http://cdsweb.cern.ch/record/1370067.
[20] ATLAS Collaboration, ATLAS-CONF-2013-021, http://cds.cern.ch/record/1525557.
[21] H.-L. Lai et al., Phys. Rev. D **82** (2010) 074024.
[22] ATLAS Collaboration, ATLAS-CONF-2012-157, http://cds.cern.ch/record/1493586.
[23] CMS Collaboration, Eur. Phys. J. C **73** 2283 (2013).
[24] CDF Collaboration, T. Aaltonen et al., Phys. Rev. Lett. **104** 101801 (2010).
[25] D0 Collaboration, V. M. Abazov et al., Phys. Rev. Lett. **108** 181803 (2012).
[26] D0 Collaboration, V. M. Abazov et al., arXiv:1304.5422 [hep-ex].
[27] ATLAS Collaboration, ATLAS-CONF-2013-020, http://cds.cern.ch/record/1525555.
[28] CDF Collaboration, T. Aaltonen at al., CDF Note 10957, http://www-cdf.fnal.gov/physics/ewk/2013/ZZ_97fb/cdf10957_ZZ97_public.pdf.
[29] ATLAS Collaboration, JHEP **1303** 128 (2013).
[30] CMS Collaboration, JHEP **1301** 063 (2013).
[31] D0 Collaboration, V. M. Abazov et al., Phys. Lett. B **718** 451 (2012).
[32] Figure from https://twiki.cern.ch/twiki/bin/view/CMSPublic/PhysicsResultsSMPaTGC.
[33] D0 Collaboration, V. M. Abazov et al., arXiv:1305.1258 [hep-ex].
[34] CMS Collaboration, arXiv:1305.5596 [hep-ex].
[35] OPAL Collaboration, G. Abbiendi et al., Phys. Rev. D **70** 032005 (2004).